Title	Enhanced efficiency of solution-processed small-molecule solar cells upon incorporation of gold nanospheres and nanorods into organic layers
Author(s)	Xu, Xiaoyan; Kyaw, Aung Ko Ko; Peng, Bo; Du, Qingguo; Hong, Lei; Demir, Hilmi Volkan; Wong, Terence Kin Shun; Xiong, Qihua; Sun, Xiao Wei
Citation	Xu, X., Kyaw, A. K. K., Peng, B., Du, Q., Hong, L., Demir, H. V., et al. (2014). Enhanced efficiency of solution-processed small-molecule solar cells upon incorporation of gold nanospheres and nanorods into organic layers. Chemical Communications, 50, 4451-4454.
Date	2014
URL	http://hdl.handle.net/10220/19832
Rights	© 2014 The Royal Society of Chemistry. This is the author created version of a work that has been peer reviewed and accepted for publication by Chemical Communications, The Royal Society of Chemistry. It incorporates referee's comments but changes resulting from the publishing process, such as copyediting, structural formatting, may not be reflected in this document. The published version is available at: [DOI: http://dx.doi.org/10.1039/C4CC01322K].

ChemComm

RSCPublishing

COMMUNICATION

Enhanced efficiency of solution-processed small-molecule solar cells by incorporating gold nanospheres and nanorods into organic layers†

Cite this: DOI: 10.1039/x0xx00000x

Received 00th January 2012,
Accepted 00th January 2012

DOI: 10.1039/x0xx00000x

www.rsc.org/

Xiaoyan Xu,[a] Aung Ko Ko Kyaw,[b] Bo Peng,[c] Qingguo Du,[d] Lei Hong,[a] Hilmi Volkan Demir,[ac] Terence, K. S. Wong,*[a] Qihua Xiong*[ac] and Xiao Wei Sun*[a]

The significantly enhanced performance by incorporation of Au nanoparticles in solution-processed small-molecule solar cells is demonstrated. Simultaneously incorporating Au nanospheres into the hole transport layer and Au-silica nanorods into the active layer achieves superior broadband absorption improvement in the device with a power conversion efficiency of 8.72% with 31% enhancement.

Solution-processed small molecule (SM) bulk heterojunction (BHJ) organic solar cells are emerging as a competitive alternative to widely studied polymer solar cells (PSC).[1] A power conversion efficiency (PCE) higher than 8% has recently been reported due to the excellent solubility in organic solvents, broadband light absorption and good charge transport property of the solution-processed SM donor.[2] Moreover, this type of SM donor offers simple synthesis, purification and monodispersity compared to polymeric materials.[1d] As with the PSC, SM solar cells are limited by insufficient light absorption because the short exciton diffusion length and low carrier mobilities of organic semiconductor materials necessitate the use of thin active layers.[3] As a result, an approach to enhance light absorption without increasing the thickness of the active layer is necessary. Recently, metallic nanoparticles (NPs) have been widely introduced into PSC for enhanced light harvesting induced by the plasmonic effect of metallic NPs.[4] In the literature, there are reports on plasmonic PSC in which single metallic NPs are incorporated into various layers, for examples: the hole transport layer (HTL),[4b] active layer[4c] or both,[4d] In addition, two different metallic NPs had been blended within a single layer.[4e, 4f] Despite significant PCE enhancement in PSC, there have been no reports on the plasmonic effect of metallic NPs in solution-processed SM solar cells. In plasmonic devices, the configuration that incorporates metallic NPs into the HTL layer and the active layer results in better hole transport and improved light absorption[4d] while the configuration that combines different shapes of NPs in the active layer achieved a broadband absorption enhancement.[4e] However, embedding NPs with two different shapes into the HTL layer and the active layer respectively, in order to leverage advantages of both configurations, has not been reported yet.

In this communication, we report high-performance solution-processed SM solar cells by incorporation of Au nanospheres into the poly(3,4-ethylene-dioxythiophene): poly(styrenesulphonate) (PEDOT:PSS) layer and Au-silica nanorods into the 7,7'-(4,4-bis(2-ethylhexyl)-4*H*-silolo[3,2-b:4,5-b']-dithiophene-2,6-diyl)bis(6-fluoro-4-(5'-hexyl-[2,2'-bithiophen]-5-yl)benzo[*c*][1,2,5]thiadiazole):[6,6]-phenyl-C_{71}-butyric acid methyl ester (p-DTS(FBTTh$_2$)$_2$:$PC_{70}BM$) layer, simultaneously. Thus far, only a few reports studied the metallic nanorods with larger size which have a longer extinction wavelength to contribute a wide absorption spectrum enhancement up to 700 nm. These nanorods can give rise to both plasmonic and scattering effects.[5] A combination of Au nanospheres and Au-silica nanorods in organic layers achieves a broader optical absorption enhancement and better hole transport. As a result, significantly improved PCE is realized by incorporating dual Au NPs.

Fig. 1a-d shows molecular structures of p-DTS(FBTTh$_2$)$_2$ and $PC_{70}BM$, SM device structure, and the transmission electron microscope (TEM) images of Au nanospheres and Au-silica nanorods, respectively. Au NPs were synthesized using the seed-mediated method.[5b, 5c] Au nanospheres had an average diameter of about 10 nm. Au-silica nanorods are completely and uniformly coated by 6 nm silica shell and have the average length and diameter of 89 nm and 34 nm respectively. The normalized UV-vis absorption spectra of Au nanospheres in water and Au-silica nanorods in chlorobenzene (CB) were measured. Fig. 1e shows that the maximum absorption peaks of Au nanospheres and Au-silica nanorods were at 521 and 681 nm, respectively. Here, four types of SM solar cells were fabricated (Device A: reference device without NPs; B: Au nanospheres in PEDOT:PSS only; C: Au-silica nanorods in the active layer only; D: NPs in both PEDOT:PSS and the active layers). The atomic force microscopy (AFM) images of the PEDOT:PSS layer and the active layer in Fig. S1, show that the root-mean-square (RMS) roughness of PEDOT:PSS films increases from 0.872 nm to 0.899 nm and that of the p-DTS(FBTTh$_2$)$_2$:$PC_{70}BM$ films increases from 1.677 nm to 1.840 nm when incorporating NPs. The almost unchanged RMS roughness confirm that all the NPs are embedded within PEDOT:PSS layer and the active layer and would not affect their morphologies.

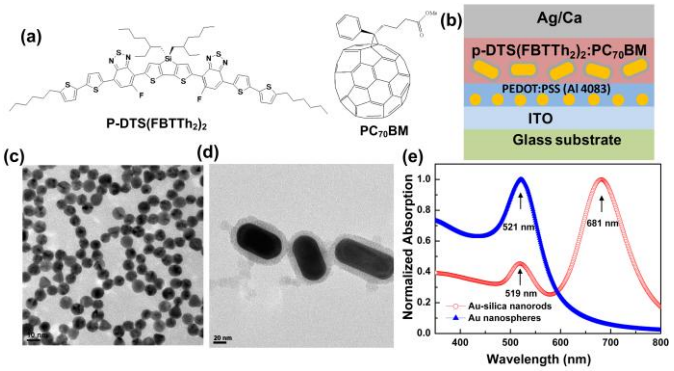

Fig. 1 (a) Molecular structures of the p-DTS(FBTTh$_2$)$_2$ and PC$_{70}$BM, (b) device structure of the SM solar cell, (c) TEM image of Au nanospheres, (d) TEM image of Au-silica nanorods and (e) normalized UV-Vis absorption spectra of Au nanospheres in water and Au-silica nanorods in CB.

The current density-voltage (*J-V*) characteristics of the four devices with Au NPs incorporated into different layers are shown in Fig. 2a. The average photovoltaic parameters from ten identical devices for each type are listed in Table 1. We first investigate the impact of Au NPs incorporated in single organic layer of SM solar cell, either in HTL or active layer at a time. Then, we studied the effect of Au NPs incorporated in all organic layers (in both HTL and active layer simultaneously). The reference device has average PCE of 6.52 ±0.15% with an open-circuit voltage (V_{OC}) of 0.77 ±0.01 V, short-circuit current density (J_{SC}) of 12.17 ±0.32 mA cm^{-2} and a fill factor (*FF*) of 69.65 ±0.65%. After incorporation of Au nanospheres only in the PEDOT:PSS layer, the V_{OC} of the plasmonic device remained the same, J_{SC} and *FF* both increased to 13.53 ±0.36 mA cm^{-2} and 71.2 ±0.79%, respectively, leading to an average PCE of 7.41 ±0.22%. Besides, the series resistance (R_S) of plasmonic device, extracted from the dark *J-V* curve, reduced from 2.75 to 2.04 Ω cm^2 which contributes to an increase of *FF*. When only Au-silica nanorods are incorporated in the active layer, V_{OC} and R_S remained the same and *FF* increased slightly to 70.58 ±0.44%. In contrast, J_{SC} has a larger enhancement to 14.96 ± 0.30 mA cm^{-2} than previous plasmonic device, which is due to the broader absorption spectrum of Au-silica nanorods that extends to longer wavelengths relative to Au nanospheres. When doping Au NPs into both the PEDOT:PSS layer and the active layer, J_{SC} and *FF* further improved to 15.56 ± 0.37 mA cm^{-2} and 71.51 ±0.75% while the V_{OC} remain unchanged, resulting in a much better PCE of 8.54 ±0.22% (with the maximum value of 8.72%).

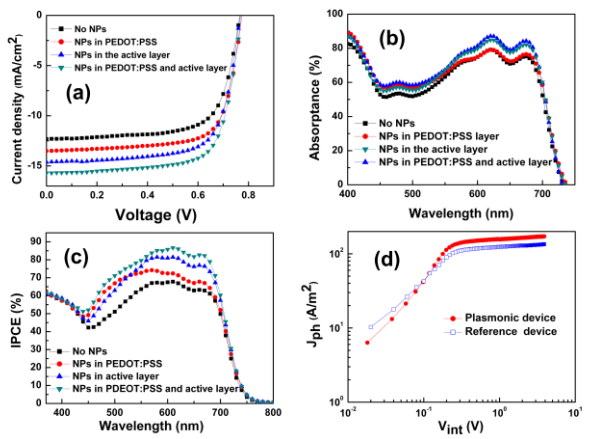

Fig. 2 (a) *J-V* characteristics of solar cells with and without NPs, (b) UV-Vis absorption spectra of p-DTS(FBTTh$_2$)$_2$:PC$_{70}$BM BHJ films with and without NPs, (c) IPCE spectra of solar cells with and without NPs and (d) photocurrent density (J_{ph}) versus internal voltage (V_{int}) characteristics of the reference device and dual NPs device.

Table 1 Photovoltaic parameters of SM BHJ devices with Au NPs in different layers under AM 1.5G illumination at 100 mW cm^{-2}.

Device	J_{SC} (mA cm^{-2})	V_{OC} (V)	*FF* (%)	PCE (%)
A	12.17 ± 0.32	0.77 ± 0.01	69.65 ± 0.65	6.52 ± 0.15
B	13.53 ± 0.36	0.77 ± 0.01	71.20 ± 0.79	7.41 ± 0.22
C	14.96 ± 0.30	0.77 ± 0.01	70.58 ± 0.44	8.11 ± 0.17
D	15.56 ± 0.37	0.77 ± 0.01	71.51 ± 0.75	8.54 ± 0.22

To verify that the improved J_{SC} is due to optical effect of Au NPs, we performed the UV-vis absorption and the incident photon to current conversion efficiency (IPCE) measurements. Fig. 2b, c shows that the absorption and IPCE spectra of the active layer are both enhanced in the spectral region of 420 to 550 nm after incorporation of Au nanospheres only in PEDOT:PSS layer, and further improvement in the spectral range of 460 to 720 nm are evident after incorporation of Au-silica nanorods only in the active layer. In addition, the broader light absorption and IPCE spectra covering from 420 to 720 nm are achieved when combining dual Au NPs in the devices. Such enhanced absorption and IPCE spectra are well matched with the plasmonic resonance region of Au nanospheres and Au-silica nanorods.

To further confirm the effect of Au NPs on the optical absorption of the SM solar cell, we determined the maximum photoinduced carrier generation rate (G_{max}) in devices with and without dual NPs.[6] Fig. 2d reveals the dependence of the photocurrent density (J_{ph}) on the internal voltage (V_{int}) for reference and plasmonic devices. J_{ph} is determined as $J_{ph} = J_L - J_D$, where J_L and J_D are the current density under illumination and in the dark, respectively. V_{int} is calculated as $V_{int} = V_0 - V_a$, where V_0 is the voltage at which $J_{ph} = 0$ and V_a is the applied voltage.[6a] Fig.3d shows that J_{ph} increases linearly at low V_{int} and saturates at a high V_{int} (2 V and above), which is large enough to dissociate all the photogenerated excitons into free charge carriers and collect them at the electrodes. Thus, at a high V_{int}, saturation current density (J_{sat}) is only limited by the total number of absorbed photons. G_{max} could be calculated from $J_{sat} = qLG_{max}$, where q is the electronic charge and L is the thickness of active layer.[6b] The value of G_{max} for the reference device and plasmonic device are 8.43 × 10^{27} m^{-3} s^{-1} (J_{sat} = 135 A m^{-2}) and 1.07 × 10^{28} m^{-3} s^{-1} (J_{sat} = 172 A m^{-2}), respectively. A significant enhancement of G_{max} occurred after incorporating dual Au NPs. Since G_{max} corresponds to the maximum number of absorbed photons, such enhancement demonstrates increased light absorption in device with dual NPs.

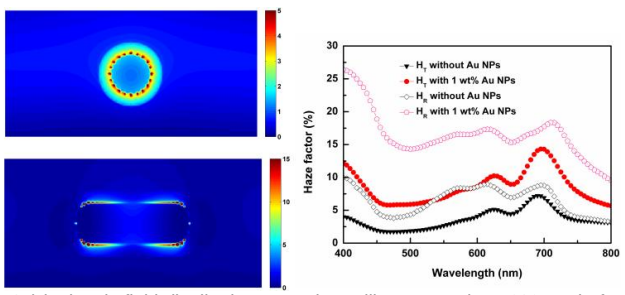

Fig. 3 (a) Electric field distribution around Au-silica nanorods at 680 nm in front view and side view and (b) Transmission haze factor and reflection spectra for p-DTS(FBTTh$_2$)$_2$:PC$_{70}$BM film with and without 1 wt% of Au–silica nanorods.

The mechanisms of enhanced light absorption by Au NPs are studied by finite-difference time-domain (FDTD) method and diffuse scattering measurements.[7] Fig. 3a shows the distribution of electric field around the Au-silica nanorods at 680 nm. It is found that the electric field is increased by a factor of 2 relative to the incident light outside the silica shell which will increase absorption within the active layer. Moreover, the haze factor spectra for transmission (H_T) and reflection (H_R) are measured by dividing the

diffuse transmission/reflection by the total transmission/reflection. Fig. 3 shows the increase in both H_T and H_R upon incorporating the Au-silica nanorods, suggesting that NPs scatter more light to increase the optical path. Therefore, both plasmonic and scattering effects excited by NPs contribute to light absorption in SM solar cell.

Fig. 4a shows the charge collection probability (P_C) versus V_{int}. The P_C could be obtained by normalizing J_{ph} by J_{sat}.[6c] The P_C under short-circuit condition (V_a = 0 V) increases from 88.1% to 91.3% by adding dual Au NPs, indicating that the incorporation of Au NPs has a positive influence on the charge collection by electrodes. The value of P_C is higher than PSCs and it decreased slowly from short-circuit condition to open-circuit condition compared to sharp increase of polymer counterpart.[8] This indicates that there is less recombination and thus result in high photocurrent and fill factor in p-DTS(FBTTh$_2$)$_2$:PC$_{70}$BM device.

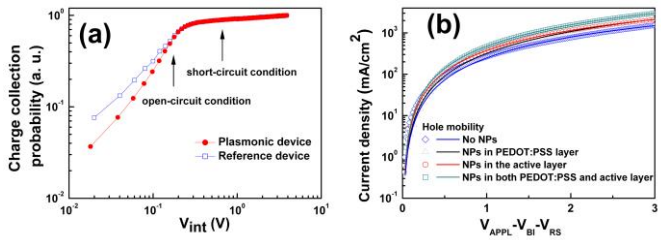

Fig. 4 (a) Charge collection probability (P_C) versus internal voltage (V_{int}) characteristics of the reference device and dual NPs device and (b) the dark *J-V* characteristics of hole-only devices with and without Au NPs.

Since carrier mobility is an important factor for charge transport and mainly limited by the hole transport in our devices,[6a] holy-only devices were fabricated to determine the hole mobility. The dark *J-V* characteristics of hole-only devices are measured and fitted using the space-charge limited current (SCLC) model and the Mott-Gurney law that includes field-dependent mobility,[9] shown in Fig. 4b. Upon incorporation of Au NPs in the PEODT:PSS layer only, active layer only and both layers, the zero field hole mobility slightly increased from 1.26 $\times 10^{-3}$ cm^2 V^{-1} s^{-1} to 1.41$\times 10^{-3}$ cm^2 V^{-1} s^{-1}, 2.07 $\times 10^{-3}$ cm^2 V^{-1} s^{-1} and 2.28 $\times 10^{-3}$ cm^2 V^{-1} s^{-1} respectively. An increase in the hole moblities indicate that the incorporation of the Au NPs does not adversely affect the charge transport in the active layer.

In conclusion, we demonstrate the maximum PCE of 8.72% with a relative performance increase of 31% in solution-processed SM solar cell by incorporation of Au nanospheres and Au-silica nanorods into organic layers. Absorption spectra, IPCE spectra and G_{max} confirm that the combination of Au NPs with two different shapes realized a broadband absorption improvement in the SM solar cells. The studied mechanisms of enhanced light absorption ascribe to both plasmonic and scattering effects by Au NPs. Enhanced carrier collection and carrier transport properties ensure the good performance in plasmonic device. Therefore, apart from contributing to light absorption within the active layer, the Au nanospheres in PEDOT:PSS layer can facilitate the hole collection and Au-silica nanorods in the active layer avoid the carrier recombination at the metal surface by insulating silica shell.

A. K. K. Kyaw thanks the Agency for Science Technology and Research (A*STAR) of Singapore for a postdoctoral fellowship. Q. X. gratefully thanks the strong support from Singapore National Research Found through a Competitive Research Program (NRF-CRP-6-2010-2), and Singapore Ministry of Education via a Tier2 grant (MOE2011-T2-2-051).

Notes and references

[a] NOVITAS, Nanoelectronics Centre of Excellence, School of Electrical and Electronic Engineering, Nanyang Technological University, Singapore 639798, Singapore. E-mail: ekswong@ntu.edu.sg, qihua@ntu.edu.sg, EXWSun@ntu.edu.sg

[b] Institute of Materials Research and Engineering (IMRE), Agency for Science Technology and Research (A*STAR), Singapore 11760, Republic of Singapore

[c] School of Physical and Mathematical Sciences, Nanyang Technological University, Singapore 639798, Singapore

[d] Institute of High Performance Computing , 1 Fusionopolis Way, #16-16 Connexis North, Singapore 138632, Republic of Singapore

† Electronic Supplementary Information (ESI) available: Synthesis of gold nanospheres, device fabrication and characterization. See DOI: 10.1039/c000000x/

1. (a) W. Cambarau, A. Viterisi, J. W. Ryan and E. Palomares, *Chem. Commun.*, 2014, DOI: 10.1039/c3cc47333c; (b) T. S. van der Poll, J. A. Love, T.-Q. Nguyen and G. C. Bazan, *Adv. Mater.*, 2012, **24**, 3646-3649; (c) Y. Sun, G. C. Welch, W. L. Leong, C. J. Takacs, G. C. Bazan and A. J. Heeger, *Nat. Mater.*, 2012, **11**, 44-48; (d) Y. Lin, Y. Li and X. Zhan, *Chem. Soc. Rev.*, 2012, **41**, 4245-4272; (e) Y. Yang, J. Zhang, Y. Zhou, G. Zhao, C. He, Y. Li, M. Andersson, O. Inganäs and F. Zhang, *J. Phys. Chem. C*, 2010, **114**, 3701-3706.
2. (a) A. K. K. Kyaw, D. H. Wang, D. Wynands, J. Zhang, T.-Q. Nguyen, G. C. Bazan and A. J. Heeger, *Nano Lett.*, 2013, **13**, 3796-3801; (b) A. K. K. Kyaw, D. H. Wang, V. Gupta, W. L. Leong, L. Ke, G. C. Bazan and A. J. Heeger, *ACS Nano*, 2013, **7**, 4569-4577.
3. S. R. Forrest, *MRS. Bull.*, 2005, **30**, 28-32.
4. (a) E. Stratakis and E. Kymakis, *Mater.Today*, 2013, **16**, 133-146; (b) J.-L. Wu, F.-C. Chen, Y.-S. Hsiao, F.-C. Chien, P. Chen, C.-H. Kuo, M. H. Huang and C.-S. Hsu, *ACS Nano*, 2011, **5**, 959-967; (c) D. H. Wang, D. Y. Kim, K. W. Choi, J. H. Seo, S. H. Im, J. H. Park, O. O. Park and A. J. Heeger, *Angew. Chem. Int. Ed.*, 2011, **50**, 5519-5523; (d) F. X. Xie, W. C. H. Choy, C. C. D. Wang, W. E. I. Sha and D. D. S. Fung, *Appl. Phys. Lett.*, 2011, **99**, 153304; (e) X. Li, W. C. H. Choy, H. Lu, W. E. I. Sha and A. H. P. Ho, *Adv. Funct. Mater.*, 2013, **23**, 2728-2735; (f) L. Lu, Z. Luo, T. Xu and L. Yu, *Nano Lett.*, 2012, **13**, 59-64.
5. (a) K. S. Lee and M. A. El-Sayed, *J. Phys. Chem. B*, 2005, **109**, 20331-20338; (b) X. Xu, A. K. K. Kyaw, B. Peng, D. Zhao, T. K. S. Wong, Q. Xiong, X. W. Sun and A. J. Heeger, *Org. Electron.*, 2013, **14**, 2360-2368; (c) T. Ming, L. Zhao, Z. Yang, H. Chen, L. Sun, J. Wang and C. Yan, *Nano Lett.*, 2009, **9**, 3896-3903.
6. (a) S. R. Cowan, A. Roy and A. J. Heeger, *Phy. Rev. B*, 2010, **82**, 245207; (b) V. D. Mihailetchi, L. J. A. Koster, J. C. Hummelen and P. W. M. Blom, *Phys. Rev. Lett.*, 2004, **93**, 216601; (c) V. D. Mihailetchi, H. X. Xie, B. de Boer, L. J. A. Koster and P. W. M. Blom, *Adv. Funct. Mater.*, 2006, **16**, 699-708.
7. (a) N. Lagos, M. M. Sigalas and E. Lidorikis, *Appl. Phys. Lett.*, 2011, **99**, 063304; (b) Y.-S. Hsiao, C.-P. Chen, C.-H. Chao and W.-T. Whang, *Org. Electron.*, 2009, **10**, 551-561.
8. M. Lenes, M. Morana, C. J. Brabec and P. W. M. Blom, *Adv. Funct. Mater.*, 2009, **19**, 1106-1111.
9. (a) C. Melzer, E. Koop, V. Mihailetchi and P. Blom, *Adv. Funct. Mater.*, 2004, **14**, 865-870; (b) P. N. Murgatroyd, *J. Phys. D: Appl. Phys.*, 1970, **3**, 151.